Received: 3 October 2021 | Revised: 27 October 2021 | Accepted: 4 November 2021

DOI: 10.1002/eom2.12167

RESEARCH ARTICLE

EcoMat FUNCTIONAL MATERIALS FOR GREEN ENERGY AND ENVIRONMENT WILEY

Reversible aqueous Zn battery anode enabled by a stable complexation adsorbent interface

Yangtao Ou[1] | **Zhao Cai**[1] | **Jindi Wang**[1] | **Renming Zhan**[1] | **Shiyu Liu**[1] | **Ziheng Lu**[2] | **Yongming Sun**[1]

[1]Wuhan National Laboratory for Optoelectronics, Huazhong University of Science and Technology, Wuhan, China

[2]Department of Materials Science and Metallurgy, University of Cambridge, Cambridge, UK

Correspondence
Ziheng Lu, Department of Materials Science and Metallurgy, University of Cambridge, Cambridge CB3 0FS, UK.
Email: zl462@cam.ac.uk
Yongming Sun, Wuhan National Laboratory for Optoelectronics, Huazhong University of Science and Technology, Wuhan 430074, China.
Email: yongmingsun@hust.edu.cn

Funding information
China Postdoctoral Science Foundation, Grant/Award Numbers: 2020T130223, 2018M640694; Innovation Fund of Wuhan National Laboratory for Optoelectronics of Huazhong University of Science and Technology

Abstract

Rechargeable aqueous Zn batteries (RAZBs) are highly promising for grid-scale energy storage systems. Nevertheless, strong water molecule adsorption on Zn electrode provokes undesired corrosion reactions and electrode polarization/dendrite growth, restricting the reversibility of Zn anode and the commercialization of RAZBs. Herein, ethylenediamine tetraacetic acid (EDTA), a typical compounding ingredient, was applied in aqueous $ZnSO_4$ electrolyte to replace the adsorbed water molecules on Zn surface and enabled a stable complexation adsorbent interface. The chemically adsorbed EDTA layer reduced the direct contact between H_2O molecules and metallic Zn, and reduced the corrosion rate to more than a half. Moreover, such adsorbent interface featuring abundant oxygen/nitrogen-based functional groups regulated Zn deposition kinetics and promoted the uniform Zn plating. As consequence, the stable complexation adsorbent interface enabled highly-reversible Zn stripping/plating behavior for 5000 h under a harsh dynamic measurement that combining eletrochemical cycling at 1 mA cm^{-2} and 0.5 mAh cm^{-2} for 72 h and resting for 24 h. The effectiveness of such complexation adsorbent interface was also verified in MnO_2||Zn full cells. The complexation interface chemistry demonstrated in this study opened up new avenues for the design of low-cost and highly reversible Zn metal electrodes towards next-generation RAZBs.

KEYWORDS

aqueous batteries, electrochemical reversibility, electrode/electrolyte interface, electrolyte additive, Zn anode

1 | INTRODUCTION

Rechargeable aqueous Zn batteries (RAZBs) are highly attractive in the field of grid-scale energy storage owing to their advantages of cost-effectiveness, eco-friendliness, and high safety.[1–6] Nevertheless, Zn metal anode faces challenges in stability and reversibility in aqueous electrolyte, as exemplified by the uncontrolled dendritic-zinc growth and undesired corrosion side reactions, which have hindered the practical popularization of RAZBs.[7–11] To meet these challenges and enhance the electrochemical performance of Zn metal electrode, various methods,

including three-dimensional structure design,[12–14] employing stable host,[15–17] surface protection,[18–22] and electrolyte engineering,[23–25] have been proposed for the recent years. Despite these exciting advances, it is still eagerly needed yet challenging to develop approaches with simple operation procedures and low-cost for practical aqueous Zn electrodes with satisfied reversibility.

Electrolyte engineering is a facile way with easy manipulation merit to improve the stability and reversibility of aqueous Zn electrodes.[26–28] Regulating the electrolyte formula, such as "water-in-salt" or hydrated eutectic electrolytes,[4,29–31] to alter the solvation structure of Zn^{2+}-ions or in-situ built solid electrolyte interphase, has provided plenty of opportunity for the development of highly reversible Zn electrodes. However, the use of these approaches may significantly increase the costs, which is undesirable for low-cost applications. This is because, the functional salts or solvents can hardly be accumulated at the electrode/electrolyte interface so that an excess of functional materials need to be involved,[32] which has severely restricted their potential for practical applications. Therefore, it is urgent to develop efficient electrolyte additive that can be enriched at the interface and uncover the underlying mechanism for the improvement and practicality of long-cycling RAZBs.

In this study, we employed a tiny amount of ethylenediamine tetraacetic acid (EDTA, 0.2 wt%) as electrolyte additive in aqueous $ZnSO_4$ electrolyte that constructed a stable complexation adsorbent interface and helped to enable highly reversible aqueous Zn metal electrode. The introduced EDTA instead of water molecules were chemically adsorbed onto Zn electrode, suppressing the corrosion reaction rate down to 43.5%. Moreover, the adsorbed EDTA layer at the interface coordinated with Zn^{2+}-ions, regulated the Zn deposition kinetics, and promoted the uniform Zn plating. The Zn||Zn symmetric cells employing $ZnSO_4$ + EDTA electrolyte displayed a stable electrochemical performance for 5000 h under a dynamic measurement that combining plating/stripping cycling at 1 mA cm^{-2} and 0.5 mAh cm^{-2} for 72 h with resting for 24 h, far better than the Zn||Zn counterpart with $ZnSO_4$ electrolyte (198 h). The MnO_2||Zn full cells with $ZnSO_4$ + EDTA electrolyte exhibited a high capacity retention of 71.6% after 500 cycles at a current density of 1 mA cm^{-2}, which outperformed that with $ZnSO_4$ electrolyte (25.5% after 500 cycles). The findings in this study not only put forward a stable complexation interface chemistry for high-performance Zn anode materials, but also suggest a facile and efficient strategy for improving the stability and reversibility of Zn metal electrodes and RAZBs.

2 | EXPERIMENTAL SECTION

2.1 | Materials Synthesis

The aqueous electrolyte in this work was prepared by dissolving 5.75 g $ZnSO_4$•$7H_2O$ and 0.03 g EDTA with deionized water to 10 ml (i.e., 0.02 wt% EDTA, 2M $ZnSO_4$ + 0.01M EDTA electrolyte). The mixture was stirred under sonication at room temperature until a clear and transparent solution was obtained. The mass concentration of EDTA was calculated by the equation: C % = $m_{EDTA}/m_{electrolyte}$, where m_{EDTA} was the mass of EDTA employed, and $m_{electrolyte}$ was the total mass of electrolyte. Zn metal foil electrode with a diameter of 12 mm and a thickness of 200 μm was washed with diluted hydrochloric acid (6 vol%) and deionized water for several times to remove the surface passivation layer. The Zn electrodes after cycling were washed with Ar-saturated deionized water and ethanol for several times, dried by Ar blowing and preserved in an Ar-filled glove box to avoid oxidation before using or characterization.

2.2 | Materials characterizations

X-ray diffraction analysis (XRD) measurements were performed on an Empyrean X-ray diffractometer with Cu Kα radiation (40 kV, 30 mA) and a 2θ ranging from 5° to 45°. Scanning electron microscope (SEM) images were obtained on a Gemini SEM 300 field-emission SEM instrument. The electron probe microanalysis (EPMA) was conducted by an EPMA-8050G electron probe microanalyzer. Optical microscopy (OM) studies were carried out on an Olympus BX53M OM with a DP27 CMOS detector. Raman characterization was carried out on a Horiba LabRAMHR800 confocal Raman microspectrometer with 532 nm of excitation.

2.3 | Electrochemical measurements

The reversibility of Zn electrodes was examined by assembling symmetric cells using CR2032-type coin cells with GF/A glass fiber separator from WHATMAN and 2M $ZnSO_4$ or 2M $ZnSO_4$ + 0.01M EDTA electrolyte (200 μl). The as-assembled cells were tested at 1–10 mA cm^{-2} and 0.5–10 mAh cm^{-2} on a NEWARE battery tester instrument. Potentiodynamic polarization curves were obtained by linear sweep voltammetry on a Biologic VMP3 electrochemical workstation at a scan rate of 20 mV s^{-1} with a three-electrode system, where a saturated calomel electrode was employed as the reference electrode, a Pt wire was emplyed as the counter electrode,

and the Zn electrode was employed as the working electrode. MnO_2 cathode was prepared by electrodepositing MnO_2 on carbon cloth substrate in 2M $ZnSO_4$ + 0.2M $MnSO_4$ electrolyte under a constant voltage of 1.8 V for 8 h.[33] MnO_2||Zn full cells were assembled in CR2032 coin-type cells with GF/A glass fiber separate from WHATMAN and 2M $ZnSO_4$ or 2M $ZnSO_4$ + 0.01M EDTA electrolytes (200 μl).

2.4 | Theoretical calculations

The quantum chemical calculation in this study was performed by density functional theory under the generalized gradient approximation. The detailed setup is in consistency with our previous work.[34–36] Briefly, the Perdew–Burke–Ernzerhof form of exchange correlation functional was chosen. The plane-wave energy cut-off was set as 520 eV for the calculation of adsorption energy while for ab initio molecular dynamics (AIMD) this value was lowered to 340 eV for efficiency. The Brillouin zone was sampled on a Monkhorst-Pack grid with a density no lower than 1000/(number of the atoms in the cell). The convergence criteria of the energy and force calculations were set to 10^{-3} eV atom^{-1} and 10^{-2} eV Å^{-1}, respectively. For AIMD studies, the temperature was kept at 300 K by a Nose-Hoover thermostat and the simulation timestep was selected as 1 fs. The total simulation length of each case was 50 ps.

3 | RESULTS AND DISCUSSIONS

Figure 1A demonstrates the plating/stripping cycling behavior of metallic Zn electrode in aqueous $ZnSO_4$ electrolyte. Water molecules are absorbed to the surface of aqueous Zn electrode, which triggers corrosion reactions between active Zn metal and water molecules, producing non-conductive zinc hydroxide sulfate (ZHS) sheets. These non-conductive ZHS would increase the electrode polarization, leading to non-uniform plating of metallic Zn, and Zn dendrites formation after repeated cycling. To stabilize the electrode/electrolyte interface, EDTA electrolyte additive was introduced in this work. As shown in Figure 1B, EDTA would be absorbed instead of water molecules, thus reducing the direct contact between active Zn and water molecules, and inhibiting corrosion side reactions. Moreover, EDTA, as a typical coordination agent with abundant oxygen/nitrogen functional groups, would be coordinated with Zn^{2+}-ions and regulate the Zn nucleation and growth to enable uniform Zn plating and consequent uniform stripping.[37–39] Taking the suppressed corrosion reaction and uniform Zn plating together, improved reversibility of Zn metal electrode can be expected in EDTA-containing electrolyte.

To investigate the chemisorption of water and EDTA molecules over Zn metal, first-principles study was first performed. The structure of absorbed water/EDTA molecules on Zn metal was demonstrated in Figure 2A–D, the adsorption energy of EDTA on Zn was turned out to be −0.73 eV, 30 meV per molecule lower than that of water (Figure 2E), suggesting a stronger adsorption ability of EDTA. Moreover, AIMD simulations were carried out on aqueous $ZnSO_4$ electrolyte near the Zn surface, as shown in Figure 2F, water molecules were absorbed on the Zn surface through chemical Zn—O bond. After 20 ps of EDTA introduction, EDTA molecule would be absorbed instead of water (Figure 2G), suggesting the thermodynamic tendency of EDTA being attached to the Zn surface in aqueous $ZnSO_4$ electrolyte. Therefore, EDTA is expected to be able to replace the absorbed water on aqueous Zn electrode. To experimentally confirm the absorbed EDTA on aqueous Zn electrode, a Zn metal electrode was immersed in a 2M $ZnSO_4$ + 0.01M EDTA

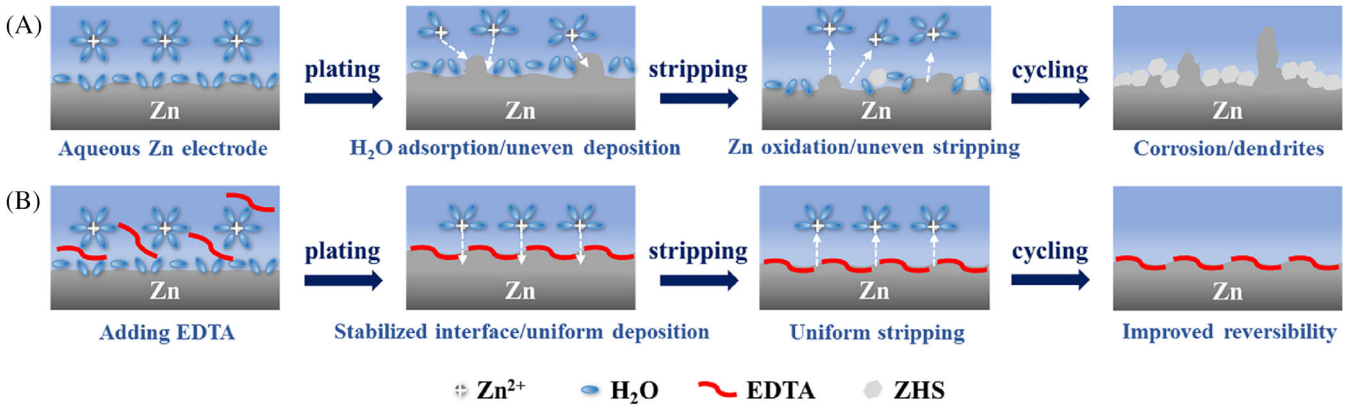

FIGURE 1 Schematic illustrations of electrochemical Zn plating/stripping cycling on Zn electrode in (A) typical $ZnSO_4$ electrolyte and (B) $ZnSO_4$ electrolyte with ethylenediamine tetraacetic acid additive

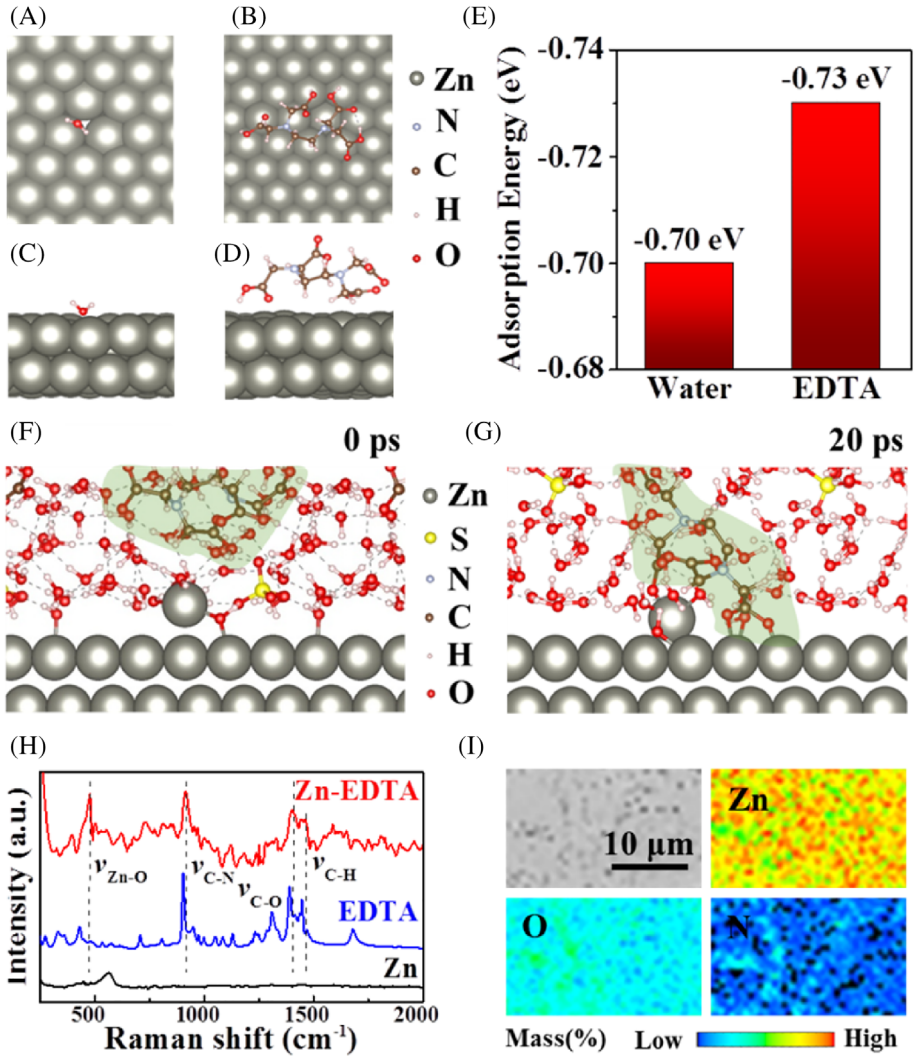

FIGURE 2 Top-view atomic configurations of (A) H_2O and (B) EDTA molecules adsorbed on Zn surfaces. Cross-section atomic configurations of (C) H_2O and (D) EDTA molecules adsorbed on Zn surfaces. (E) Adsorption energies of H_2O and EDTA molecules on Zn surface. Snapshots of AIMD simulations of aqueous $ZnSO_4$ electrolyte with EDTA addition in the vicinity of the Zn surfaces after (F) 0 ps and (G) 20 ps, suggesting the rapid adsorption of EDTA on aqueous Zn surfaces. (H) Raman spectrum of Zn electrode, EDTA powder, and Zn electrode after soaking in $ZnSO_4$ electrolyte with EDTA additives (Zn-EDTA). (I) EPMA results of the Zn electrode after soaking in $ZnSO_4$ electrolyte with EDTA additive, suggesting the successful adsorption of EDTA on Zn electrode. AIMD, ab initio molecular dynamics; EDTA, ethylenediamine tetraacetic acid; EPMA, electron probe microanalysis

solution (denoted as "Zn-EDTA") and Raman spectroscopic study was carried out. Pristine Zn electrode and EDTA powder were also studied as references. As demonstrated in Figure 2H, the Raman vibrations of C—N, C—O, C—H of EDTA molecules for Zn-EDTA were red-shifted compared to that for EDTA powder reference.[17,40] Notably, a new Raman mode at 474 cm^{-1} was found for Zn-EDTA, which was assigned to the Zn—O vibration,[40] suggesting the chemical adsorption of EDTA on Zn metal, in agreement with the calculation findings (Figure 2A–G). EPMA of Zn-EDTA electrode showed distinct O and N elemental signals (Figure 2I), further confirming the successful adsorption of EDTA on Zn metal surface.

The adsorption of EDTA could reduce the direct contact between active Zn and water, thus suppressing the corrosion side reactions. We studied the corrosion behavior of Zn electrode in 2M $ZnSO_4$ and 2M $ZnSO_4$ + 0.01M EDTA electrolyte by SEM, respectively. In contrast to a flat and clean surface for the pristine Zn metal electrode (Figure S1), the Zn metal electrode after resting in 2M $ZnSO_4$ electrolyte for 3 days exhibited a rough surface with a large number of hexagonal mircosheet corrosion products (Figure 3A and Figure S2A). Impressively, the Zn metal electrode resting in 2M $ZnSO_4$ + 0.01M EDTA electrolyte for 3 days showed a relatively flat surface with similar morphology to the pristine Zn electrode (Figure 3B, Figures S2B and S1), indicating the suppressed corrosion behavior. The different corrosion behaviors of Zn metal electrode in 2M $ZnSO_4$ and 2M $ZnSO_4$ + 0.01M EDTA electrolytes were also confirmed by XRD, the Zn metal electrode after resting in 2M $ZnSO_4$ electrolyte for 3 days showed significant diffraction of layered ZHS corrosion products (Figure 3C), following the sheet-like products in SEM (Figure 3A). On the contrast, the Zn metal electrode after resting in 2M $ZnSO_4$ + 0.01M EDTA electrolyte for 3 days showed no obvious diffraction peak of such ZHS corrosion products. To quantitatively analyze the corrosion rate of Zn metal in different electrolyte, linear polarization measurements

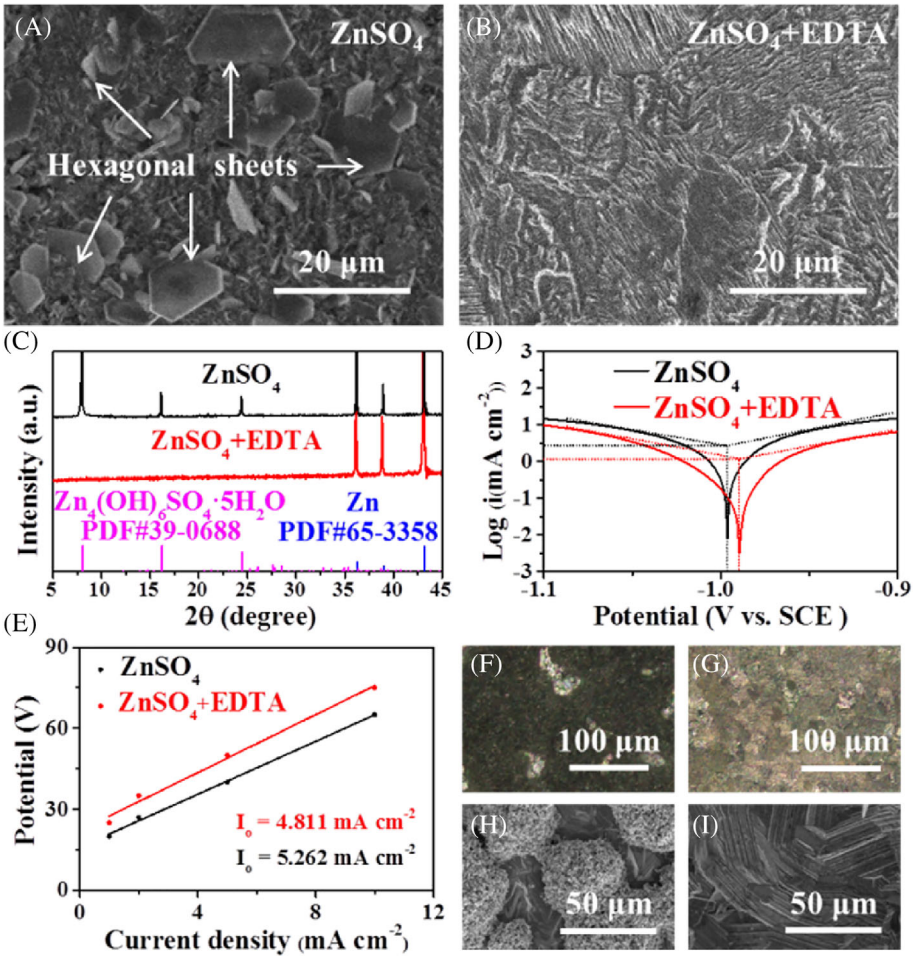

FIGURE 3 SEM images of Zn electrode after resting in (A) 2M $ZnSO_4$ electrolyte and (B) 2M $ZnSO_4$ + 0.01M EDTA electrolyte for 3 days. (C) XRD results of Zn electrode after resting in 2M $ZnSO_4$ or 2M $ZnSO_4$ + 0.01M EDTA electrolyte for 3 days. (D) Corrosion potentials and current densities of the Zn electrode in 2M $ZnSO_4$ and 2M $ZnSO_4$ + 0.01M EDTA electrolyte. (E) Exchange current density of Zn||Zn asymmetric cell with 2M $ZnSO_4$ electrolyte or 2M $ZnSO_4$ + 0.01M EDTA electrolyte. OM images of Zn electrode after plating 10 mAh cm^{-2} of Zn metal in (F) 2M $ZnSO_4$ electrolyte and (G) 2M $ZnSO_4$ + 0.01M EDTA electrolyte. SEM images of Zn electrode after plating 10 mAh cm^{-2} of Zn metal in (H) 2M $ZnSO_4$ electrolyte and (I) 2M $ZnSO_4$ + 0.01M EDTA electrolyte. EDTA, ethylenediamine tetraacetic acid; SEM, scanning electron microscope; XRD, X-ray diffraction analysis

were applied. As indicated in Figure 3D, the Zn metal electrode in 2M $ZnSO_4$ + 0.01M EDTA electrolyte showed a higher corrosion potential of −0.989 V than that in 2M $ZnSO_4$ (−0.996 V). Furthermore, the corrosion current density of Zn metal electrode in 2M $ZnSO_4$ + 0.01 M EDTA electrolyte (1.18 mA cm^{-2}) was lower than one-half of that in 2M $ZnSO_4$ (2.71 mA cm^{-2}), demonstrating a significant lower corrosion rate of Zn electrode in $ZnSO_4$ + EDTA electrolyte.

It is noted that the EDTA adsorbent layer is rich in oxygen/nitrogen-based functional groups that can be coordinated with Zn^{2+}-ions, thus regulating the Zn deposition kinetics and promoting the uniform Zn plating. The exchange current density was evaluated to investigate the Zn deposition kinetics. As demonstrated in Figure 3E and Figure S3, the Zn electrode in 2M $ZnSO_4$ + 0.01M EDTA electrolyte showed a lower exchange current density of 4.811 mA cm^{-2} than that in 2M $ZnSO_4$ electrolyte (5.262 mA cm^{-2}), suggesting a lower deposition kinetic in $ZnSO_4$ electrolyte with EDTA additive, which should be beneficial for uniform Zn plating.[41] We further studied the Zn plating process in different electrolytes using both OM and SEM. The Zn electrode after plating 10 mAh cm^{-2} of metallic Zn in 2M $ZnSO_4$ electrolyte showed a dark and rough surface under OM, implying the porous Zn deposits (Figure 3F). The SEM image of such electrode verified the non-uniform deposition (Figure 3H, Figures S4 and S5A), from which porous Zn spherical deposits with a diameter of 30 μm were observed. However, the Zn deposits in 2M $ZnSO_4$ + 0.01M EDTA electrolyte showed a flat surface with metallic luster under OM (Figure 3G), and a dense and uniform Zn plating morphology under SEM (Figure 3I and Figure S5B). It should be noted that the proportion of intensity for the (002) and (101) diffraction peaks for Zn electrodes after plating 10 mAh cm^{-2} of metallic Zn in 2M $ZnSO_4$ + 0.01M EDTA electrolyte was 0.18, which was quite different from that in 2M $ZnSO_4$ electrolyte and the pristine Zn electrode (Figure S6 and Table S1), suggesting the (101)-oriented Zn deposition in 2M $ZnSO_4$ + 0.01M EDTA electrolyte, as well as the important role of the adsorbed EDTA layer in regulating the Zn deposition behavior of Zn metal electrode. These microscopic and XRD results suggested the uniform Zn plating behavior guided by the EDTA complexation adsorbent layer.

The suppressed corrosion and uniform Zn plating behavior in $ZnSO_4$ + EDTA electrolyte should improve the stability and reversibility of Zn electrode. The effect of EDTA concentration on the overpotential and cycling stability of Zn electrode in $ZnSO_4$ electrolyte was studied. As indicated in Figures S7 and S8, at 1 mA cm^{-2} and 0.5 mAh cm^{-2}, the Zn metal electrode in 2M $ZnSO_4$ + 0.01M EDTA electrolyte exhibited a relatively low overpotential of 25 mV and the longest cycle life of 5000 h among the most of Zn metal electrodes in recent publications (Table S2). In contrast, the Zn electrode in 2M $ZnSO_4$ electrolyte showed a short cycle life of ~200 h at 1 mA cm^{-2} and 0.5 mAh cm^{-2} (Figure S9), which in turn demonstrated the advantages of EDTA additives. Thereafter, 2M $ZnSO_4$ + 0.01M EDTA electrolyte was employed in this work. Zn||Zn symmetric cells were further cycled at higher current densities and areal capacities. As demonstrated in Figure S10, at 2 mA cm^{-2} and 2 mAh cm^{-2}, the Zn electrode in 2M $ZnSO_4$ + 0.01M EDTA electrolyte exhibited stable cycling behavior with an average overpotential of 30 mV for 600 h, far better than the Zn electrode in 2M $ZnSO_4$ electrolyte (28 mV, 20 h). Even at ultrahigh current density of 10 mA cm^{-2} and areal capacity of 10 mAh cm^{-2}, the Zn electrode in 2M $ZnSO_4$ + 0.01M EDTA electrolyte (58 mV, 100 h) also outperformed that in 2M $ZnSO_4$ electrolyte (50 mV, 25 h, Figure S11). Considering the actual usage situation of battery anodes, we performed dynamic measurement combining stripping/plating cycling at 1 mA cm^{-2} and 0.5 mAh cm^{-2} for 72 h and resting for 24 h, and looping. As shown in Figure 4A, the Zn electrode in 2M $ZnSO_4$ + 0.01M EDTA electrolyte exhibited excellent electrochemical stability for 5000 h, whereas that in 2M $ZnSO_4$ electrolyte showed a significant shorter cycle life of 198 h. The Zn electrodes after 198 h of cycling in different electrolytes were examined by SEM. As demonstrated in Figure 4B, the Zn electrode in 2M $ZnSO_4$ electrolyte showed a rough and non-uniform surface with significant hexagonal ZHS sheet corrosion products, indicating a low stability and reversibility. As a comparison, the Zn electrode in 2M $ZnSO_4$ + 0.01M EDTA electrolyte showed a homogeneous surface with little ZHS (Figure 4C), suggesting the improved reversibility of such electrode. Moreover, the Zn electrode after 198 h of

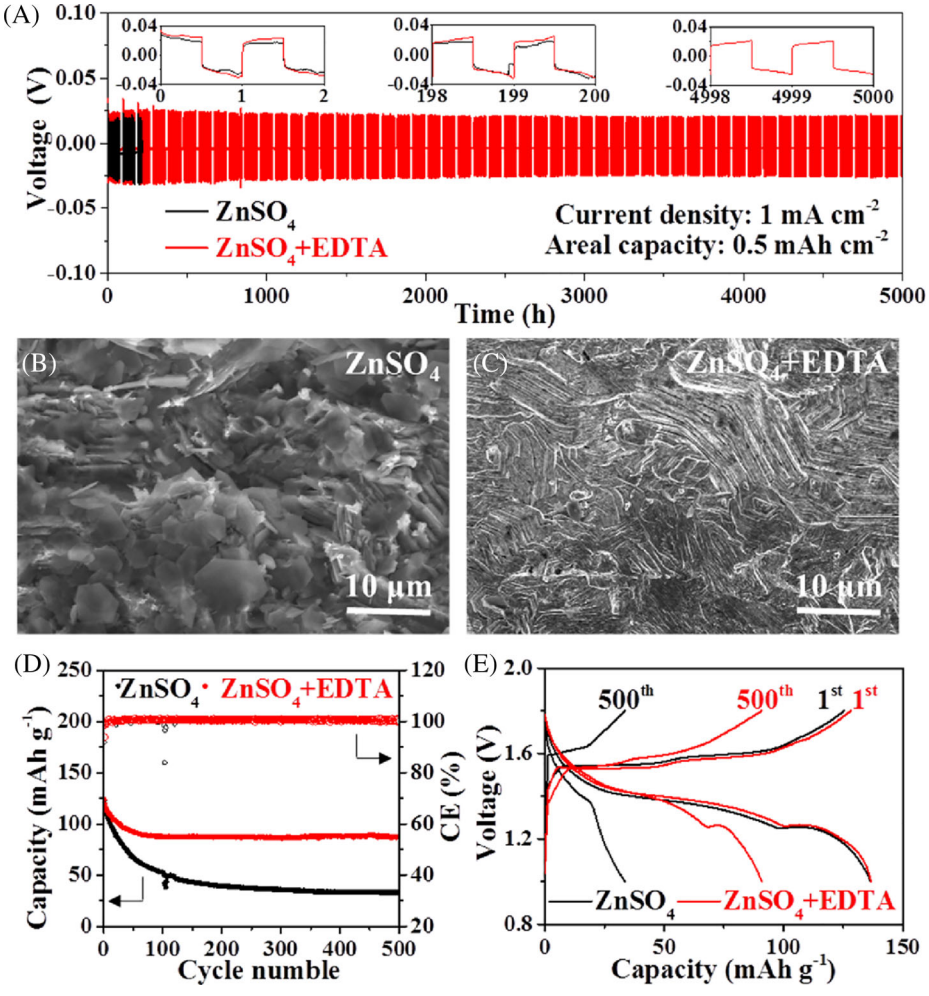

FIGURE 4 (A) Dynamic measurement combining plating/stripping cycling at 1 mA cm^{-2} and 0.5 mAh cm^{-2} for 72 h and resting for 24 h for Zn||Zn symmetric cells with 2M $ZnSO_4$ electrolyte or 2M $ZnSO_4$ + 0.01M EDTA electrolyte. SEM images of Zn electrode after cycling at 1 mA cm^{-2} and 0.5 mAh cm^{-2} for 198 h in (B) 2M $ZnSO_4$ electrolyte and (C) 2M $ZnSO_4$ + 0.01M EDTA electrolyte. (D) Cycling performance and (E) charge/discharge curves of the MnO_2||Zn full cells with 2M $ZnSO_4$ electrolyte or 2M $ZnSO_4$ + 0.01M EDTA electrolyte at 1 mA cm^{-2}. EDTA, ethylenediamine tetraacetic acid; SEM, scanning electron microscope

cycling exhibited significant diffraction peaks of ZHS corrosion products (Figure S12), while the Zn metal electrode in 2M $ZnSO_4$ + 0.01M EDTA electrolyte showed no such ZHS diffraction peaks, in accord with the SEM studies in Figure 4B,C. The excellent electrochemical reversibility of Zn in $ZnSO_4$ + EDTA electrolyte was also verified in full cells with MnO_2 cathodes. As demonstrated in Figure 4D,E, both the MnO_2||Zn full cells with 2M $ZnSO_4$ and 2M $ZnSO_4$ + 0.01M EDTA electrolyes delivered an initial capacity of 130 mAh g^{-1} at 1 mA cm^{-2}. However, the MnO_2||Zn full cell with 2M $ZnSO_4$ + 0.01M EDTA electrolyte showed a capacity retention of 71.6% after 500 cycles, which was significant higher than that with 2M $ZnSO_4$ electrolyte (only 25.5% under the same test conditions), demonstrating high practicability of EDTA electrolyte additive for aqueous Zn battery anodes.

4 | CONCLUSIONS

In summary, a highly reversible Zn metal electrode was realized by constructing a stable complexation adsorbent interface using 0.2 wt% EDTA additive in $ZnSO_4$ electrolyte. The chemically adsorbed EDTA not only reduced the corrosion rate of aqueous Zn electrode from 2.71 mA cm^{-2} to 1.18 mA cm^{-2}, but also facilitated the dendrite-free Zn plating by regulating the Zn deposition kinetics. The complexation adsorbent interface therefore ensured an improved reversibility of aqueous Zn metal electrode in both Zn||Zn symmetric cell and MnO_2||Zn full cell configurations. This work not only demonstrated the importance of constructing stable complexation adsorbent interface for high-performance Zn metal anodes, but also suggested a scalable, cost-effective, easy manipulating way to improve the reversibility of aqueous Zn electrodes, shedding light on the target development of long-cycling RAZBs.

ACKNOWLEDGMENTS

Yangtao Ou and Zhao Cai contributed equally to this work. Yongming Sun acknowledges the financial support by the Innovation Fund of Wuhan National Laboratory for Optoelectronics of Huazhong University of Science and Technology. Zhao Cai thanks the China Postdoctoral Science Foundation (No. 2018M640694, 2020T130223). The authors would like to thank the Analytical and Testing Center of Huazhong University of Science and Technology as well as the Center for Nanoscale Characterization & Devices of Wuhan National Laboratory for Optoelectronics for providing the facilities to conduct the characterization.

AUTHOR CONTRIBUTIONS

Y. Ou, Z. Cai, Z. Lu, and Y. Sun conceived the project. Y. Ou, Z. Cai, J. Wang, R. Zhan, and S. Liu performed the experiments. Z. Lu performed the computational work. Y. Ou, Z. Cai, Z. Lu, and Y. Sun wrote the manuscript. Z. Lu, and Y. Sun supervised the project. All the authors discussed the results and commented on the manuscript.

CONFLICT OF INTEREST

The authors declare no conflict of interest.

ORCID

Yongming Sun https://orcid.org/0000-0001-8528-525X

REFERENCES

1. Cao L, Li D, Pollard T, et al. Fluorinated interphase enables reversible aqueous zinc battery chemistries. *Nat Nanotech*. 2021;16(8):902-910.
2. Hao J, Li X, Zeng X, Li D, Mao J, Guo Z. Deeply understanding the Zn anode behaviour and corresponding improvement strategies in different aqueous Zn-based batteries. *Energ Environ Sci*. 2020;13(11):3917-3949.
3. Zheng J, Zhao Q, Tang T, et al. Reversible epitaxial electrodeposition of metals in battery anodes. *Science*. 2019;366(6465):645-648.
4. Wang F, Borodin O, Gao T, et al. Highly reversible zinc metal anode for aqueous batteries. *Nat Mater*. 2018;17(6):543-549.
5. Liu H, Zhu J, Tian D, et al. 3D lattice-matching layered hydroxide heterostructure with improved interfacial charge transfer and ion diffusion for high energy density supercapacitor. *Adv Mater Interfaces*. 2021;14:2100429.
6. Huang J, Zhou J, Liang S. Guest pre-intercalation strategy to boost the electrochemical performance of aqueous zinc-ion battery cathodes. *Acta Phys Chim Sin*. 2021;37:2005020.
7. Li Q, Zhao Y, Mo F, et al. Dendrites issues and advances in Zn anode for aqueous rechargeable Zn-based batteries. *EcoMat*. 2020;2(3):e12035.
8. Liu C, Xie X, Lu B, Zhou J, Liang S. Electrolyte strategies toward better zinc-ion batteries. *ACS Energy Lett*. 2021;6(3):1015-1033.
9. Song J, Xu K, Liu N, Reed D, Li X. Crossroads in the renaissance of rechargeable aqueous zinc batteries. *Mater Today*. 2021;45:191-212.
10. Yang Q, Li Q, Liu Z, et al. Dendrites in Zn-based batteries. *Adv Mater*. 2020;32(48):2001854.
11. Zheng J, Archer LA. Controlling electrochemical growth of metallic zinc electrodes: toward affordable rechargeable energy storage systems. *Sci Adv*. 2021;7(2):eabe0219.
12. Liu B, Wang S, Wang Z, Lei H, Chen Z, Mai W. Novel 3D nanoporous Zn–Cu alloy as long-life anode toward high-voltage double electrolyte aqueous zinc-ion batteries. *Small*. 2020;16(22):2001323.
13. Wang J, Cai Z, Xiao R, et al. A chemically polished zinc metal electrode with a ridge-like structure for cycle-stable aqueous batteries. *ACS Appl Mater Interfaces*. 2020;12(20):23028-23034.
14. Xiao R, Cai Z, Zhan R, et al. Localizing concentrated electrolyte in pore geometry for highly reversible aqueous Zn metal batteries. *Chem Eng J*. 2021;420:129642.

15. Jian Q, Wan Y, Sun J, Wu M, Zhao T. A dendrite-free zinc anode for rechargeable aqueous batteries. *J Mater Chem A*. 2020;8(38):20175-20184.
16. Yin Y, Wang S, Zhang Q, et al. Dendrite-free zinc deposition induced by tin-modified multifunctional 3D host for stable zinc-based flow battery. *Adv Mater*. 2020;32(6):1906803.
17. Zhang Q, Luan J, Fu L, et al. The three-dimensional dendrite-free zinc anode on a copper mesh with a zinc-oriented polyacrylamide electrolyte additive. *Angew Chem Int Ed*. 2019;58(44):15841-15847.
18. Cai Z, Ou Y, Wang J, et al. Chemically resistant Cu–Zn/Zn composite anode for long cycling aqueous batteries. *Energy Storage Mater*. 2020;27:205-211.
19. Cai Z, Ou Y, Zhang B, et al. A replacement reaction enabled interdigitated metal/solid electrolyte architecture for battery cycling at 20 mA cm^{-2} and 20 mAh cm^{-2}. *J Am Chem Soc*. 2021;143(8):3143-3152.
20. Han J, Euchner H, Kuenzel M, et al. A thin and uniform fluoride-based artificial interphase for the zinc metal anode enabling reversible Zn/MnO_2 batteries. *ACS Energy Lett*. 2021;6(9):3063-3071.
21. Ma L, Li Q, Ying Y, et al. Toward practical high-areal-capacity aqueous zinc-metal batteries: quantifying hydrogen evolution and a solid-ion conductor for stable zinc anodes. *Adv Mater*. 2021;33(12):2007406.
22. Miao Z, Du M, Li H, et al. Constructing nano-channeled tin layer on metal zinc for high-performance zinc-ion batteries anode. *EcoMat*. 2021;3(4):e12125.
23. Jin S, Zhang D, Sharma A, et al. Stabilizing zinc electrodeposition in a battery anode by controlling crystal growth. *Small*. 2021;17(33):2101798.
24. Luo M, Wang C, Lu H, et al. Dendrite-free zinc anode enabled by zinc-chelating chemistry. *Energy Storage Mater*. 2021;41:515-521.
25. Sun P, Ma L, Zhou W, et al. Simultaneous regulation on solvation shell and electrode interface for dendrite-free Zn ion batteries achieved by a low-cost glucose additive. *Angew Chem Int Ed*. 2021;60(33):18247-18255.
26. Cao L, Li D, Hu E, et al. Solvation structure design for aqueous Zn metal batteries. *J Am Chem Soc*. 2020;142(51):21404-21409.
27. Guo S, Qin L, Zhang T, et al. Fundamentals and perspectives of electrolyte additives for aqueous zinc-ion batteries. *Energy Storage Mater*. 2021;34:545-562.
28. Hao J, Long J, Li B, et al. Toward high-performance hybrid Zn-based batteries via deeply understanding their mechanism and using electrolyte additive. *Adv Funct Mater*. 2019;29(34):1903605.
29. Wu X, Xu Y, Zhang C, et al. Reverse dual-ion battery via a $ZnCl_2$ water-in-salt electrolyte. *J Am Chem Soc*. 2019;141(15):6338-6344.
30. Yang W, Du X, Zhao J, et al. Hydrated eutectic electrolytes with ligand-oriented solvation shells for long-cycling zinc-organic batteries. *Joule*. 2020;4(7):1557-1574.
31. Zhang C, Holoubek J, Wu X, et al. A $ZnCl_2$ water-in-salt electrolyte for a reversible Zn metal anode. *Chem Commun*. 2018;54(100):14097-14099.
32. Cao Z, Zhuang P, Zhang X, Ye M, Shen J, Ajayan PM. Strategies for dendrite-free anode in aqueous rechargeable zinc ion batteries. *Adv Energy Mater*. 2020;10(30):2001599.
33. Sun W, Wang F, Hou S, et al. Zn/MnO_2 battery chemistry with H^+ and Zn^{2+} coinsertion. *J Am Chem Soc*. 2017;139(29):9775-9778.
34. Chen J, Yang Z, Liu G, et al. Reinforcing concentrated phosphate electrolytes with in-situ polymerized skeletons for robust quasi-solid lithium metal batteries. *Energy Storage Mater*. 2020;25:305-312.
35. Wan TH, Lu Z, Ciucci F. A first principle study of the phase stability, ion transport and substitution strategy for highly ionic conductive sodium antipervoskite as solid electrolyte for sodium ion batteries. *J Power Sources*. 2018;390:61-70.
36. Liu J, Lu Z, Effat MB, Ciucci F. A theoretical study on the stability and ionic conductivity of the $Na_{11}M_2PS_{12}$ (M = Sn, Ge) superionic conductors. *J Power Sources*. 2019;409:94-101.
37. Jin YQ, Chen H, Peng L, et al. Interfacial polarization triggered by glutamate accelerates dehydration of hydrated zinc ions for zinc-ion batteries. *Chem Eng J*. 2021;416:127704.
38. Lu H, Zhang X, Luo M, et al. Amino acid-induced interface charge engineering enables highly reversible Zn anode. *Adv Funct Mater*. 2021;45:2103514.
39. Zou K, Cai P, Deng X, et al. Highly stable zinc metal anode enabled by oxygen functional groups for advanced Zn-ion supercapacitors. *Chem Commun*. 2021;57(4):528-531.
40. Mitha A, Yazdi AZ, Ahmed M, Chen P. Surface adsorption of polyethylene glycol to suppress dendrite formation on zinc anodes in rechargeable aqueous batteries. *ChemElectroChem*. 2018;5(17):2409-2418.
41. Xie X, Liang S, Gao J, et al. Manipulating the ion-transfer kinetics and interface stability for high-performance zinc metal anodes. *Energ Environ Sci*. 2020;13(2):503-510.

SUPPORTING INFORMATION

Additional supporting information may be found in the online version of the article at the publisher's website.

How to cite this article: Ou Y, Cai Z, Wang J, et al. Reversible aqueous Zn battery anode enabled by a stable complexation adsorbent interface. *EcoMat*. 2021;e12167. doi:10.1002/eom2.12167